

## 2D NMR Exchange Spectroscopy with Spy Nuclei for Thallium(III) Cyano Complexes in Aqueous Solution

Gyula Batta,<sup>1a</sup> István Bányai,<sup>1b</sup> and Julius Glaser\*

Contribution from the Department of Inorganic Chemistry, The Royal Institute of Technology (KTH), S-100 44 Stockholm, Sweden

Received November 2, 1992

**Abstract:** We have used a combination of <sup>13</sup>C and <sup>205</sup>Tl NMR 2D exchange spectroscopy (EXSY) to study cyanide exchange reactions in an aqueous solution containing the recently established complexes Tl(<sup>13</sup>CN)<sub>3</sub> and Tl(<sup>13</sup>CN)<sub>4</sub><sup>-</sup>, and H<sup>13</sup>CN. Because of the well-resolved heteronuclear spin-spin couplings (up to 8 kHz), the system was considered to have six exchanging sites for <sup>13</sup>C NMR and nine for <sup>205</sup>Tl NMR. The employed method gave an overview of the dynamic processes at chemical equilibrium. It is shown that in such systems otherwise invisible kinetic information can be brought into light. The EXSY spectra were evaluated quantitatively for both nuclei, and rate constants were calculated for the different exchange pathways.

One- and two-dimensional NMR exchange spectroscopy has become a powerful tool for studying slow and intermediate chemical exchange processes.<sup>2-7</sup> Both 1D selective magnetization-transfer<sup>2</sup> and 2D EXSY<sup>3</sup> methods can provide mapping of exchange pathways and even give rate constants for specific chemical reactions. The 2D EXSY method has recently been applied to study kinetic problems in inorganic chemistry, using, e.g., <sup>119</sup>Sn,<sup>7ab</sup> <sup>51</sup>V,<sup>7c</sup> and <sup>7</sup>Li NMR.<sup>7d</sup>

Information about dynamics of aluminium group elements in solution is scarce. Solvent exchange mechanisms for aluminium, gallium, and indium have been studied by the research groups of van Eldik,<sup>8a</sup> Merbach,<sup>8b</sup> and Tanaka.<sup>8c</sup> The knowledge about dynamic properties of thallium(III) in solution is more limited. For solvent exchange, there are only two recent papers dealing with the water exchange rate for the hydrated Tl(III) ion.<sup>9</sup>

Recently, we have established the formation and redox stability of cyanothallium(III) complexes<sup>10</sup> and of the species Tl(SCN)<sub>2</sub><sup>+</sup>

in aqueous solution.<sup>11</sup> Continuing our work on the chemistry of Tl(III), we here report a study of dynamics of the Tl<sup>3+</sup>-CN<sup>-</sup> system in aqueous solution using <sup>205</sup>Tl and <sup>13</sup>C NMR. We show that in special spin systems with well-resolved heteronuclear spin-spin couplings, otherwise invisible dynamic information can be brought into light. This is the so-called "spy nucleus" approach, which was used previously by Ernst et al. and recently by Ball et al. in a different context.<sup>12</sup> We analyze quantitatively the kinetics of cyanide exchange for the thallium(III) cyanide complexes in aqueous solution by using a combination of <sup>13</sup>C NMR 2D EXSY and, for the first time, <sup>205</sup>Tl 2D EXSY technique.

### Experimental Section

**Preparation and Analysis of Solutions.** An aqueous solution containing exclusively the species Tl(CN)<sub>3</sub>, Tl(CN)<sub>4</sub><sup>-</sup>, and HCN in a concentration ratio 0.021:0.018:0.166 M was prepared as previously,<sup>10</sup> by adding <sup>13</sup>C-enriched solid Na<sup>13</sup>CN to a solution of Tl(ClO<sub>4</sub>)<sub>3</sub> in HClO<sub>4</sub>. The ionic strength was kept by LiClO<sub>4</sub> and NaClO<sub>4</sub> so that [ClO<sub>4</sub><sup>-</sup>] = 4 M, [Li<sup>+</sup>] = 3 M, [Na<sup>+</sup>] = 1 M, and [H<sup>+</sup>] = 0.17 M. The solution contained ~95% <sup>13</sup>C, and the solvent was H<sub>2</sub>O/D<sub>2</sub>O = 95:5. The solution was kept dark and cold to avoid decomposition. The solution of concentrated acidic Tl(ClO<sub>4</sub>)<sub>3</sub> was prepared by anodic oxidation of TlClO<sub>4</sub>.<sup>13</sup>

Analysis of Tl(III), Tl(I), and H<sup>+</sup> in the Tl(ClO<sub>4</sub>)<sub>3</sub> stock solution was performed in the same way as described earlier.<sup>10</sup> Tl(I) and (after reduction with SO<sub>2</sub>) Tl(III) concentrations were determined by titration with KBrO<sub>3</sub> and the acidity by titration with NaOH.

**NMR Measurements.** All NMR spectra were recorded with a Bruker AM400 spectrometer at a probe temperature of 25 (±0.5) °C using a Eurotherm temperature regulator. The samples were contained in 10-mm outer-diameter sample tubes, and the spectra were recorded in deuterium locked mode. A standard NOESY pulse sequence provided with the spectrometer was used for the 2D experiments. NMR parameters were chosen in order to obtain approximately quantitative spectra. Typical values for <sup>205</sup>Tl NMR: spectrometer frequency (SF) = 230.8 MHz, spectral window (SW) = 70 kHz, flip angle ~90° (36 μs), relaxation delay time ~0.3 s, digital resolution (DR) = 30-70 Hz/point, number of scans (NS) = 512. The chemical shift values are referred in ppm toward higher frequency from the <sup>205</sup>Tl NMR signal of an aqueous solution of Tl<sup>+</sup>ClO<sub>4</sub>, extrapolated to infinite dilution. Since the chemical shifts of aqueous solutions of different Tl(I) salts extrapolate to the same value at infinite dilution,<sup>14</sup> this value corresponds to the chemical shift of the free hydrated Tl<sup>+</sup> ion. For <sup>13</sup>C NMR: SF = 100.6 MHz, SW = 8 kHz,

\* To whom correspondence should be addressed.

(1) Permanent address: L. Kossuth University, H-4010 Debrecen, Hungary.

(a) Research Group for Antibiotics of the Hungarian Academy of Sciences. (b) Department of Physical Chemistry.

(2) (a) Forsén, S.; Hoffman, R. A. *J. Chem. Phys.* **1963**, *39*, 2892. (b) Campbell, I. D.; Dobson, C. M.; Ratcliffe, R. G.; Williams, R. J. P. *J. Magn. Reson.* **1978**, *29*, 397. (c) Perrin, C. L.; Johnstone, E. R. *J. Magn. Reson.* **1979**, *33*, 619. (d) Bellon, S. F.; Chen, D.; Johnstone, E. R. *J. Magn. Reson.* **1987**, *73*, 168. (e) Perrin, C. L.; Engler, R. E. *J. Magn. Reson.* **1990**, *90*, 363. (f) Engler, R. E.; Johnstone, E. R.; Wade, C. G. *J. Magn. Reson.* **1988**, *77*, 377.

(3) (a) Jeener, J.; Meier, B. H.; Bachmann, P.; Ernst, R. R. *J. Chem. Phys.* **1979**, *71*, 4546. (b) Macura, S.; Ernst, R. R. *Mol. Phys.* **1980**, *41*, 95.

(4) (a) Willem, R. *Prog. Nucl. Magn. Reson. Spectrosc.* **1987**, *20*, 1. (b) Perrin, C. R.; Dwyer, T. *J. Chem. Rev.* **1990**, *90*, 935. (c) Orrell, K. G.; Sik, V.; Stephenson, D. *Prog. Nucl. Magn. Reson. Spectrosc.* **1990**, *22*, 141.

(5) (a) Perrin, C. L.; Gipe, R. K. *J. Am. Chem. Soc.* **1984**, *106*, 4036. (b) Keepers, J. W.; James, T. L. *J. Magn. Reson.* **1984**, *57*, 404. (c) Bremer, J.; Mendz, G. L.; Moore, W. J. *J. Am. Chem. Soc.* **1984**, *106*, 4691.

(6) (a) Johnstone, E. R.; Dellwo, M. J.; Hendrix, J. *J. Magn. Reson.* **1986**, *66*, 399. (b) Olejniczak, E. T.; Gampe, R. T., Jr.; Fesik, S. W. *J. Magn. Reson.* **1986**, *67*, 26. (c) Abel, E. W.; Coston, T. P. J.; Orrell, K. G.; Sik, V.; Stephenson, D. *J. Magn. Reson.* **1986**, *70*, 3.

(7) (a) Ramachandran, R.; Knight, C. T. G.; Kirkpatrick, R. J.; Olfield, E. *J. Magn. Reson.* **1985**, *65*, 136. (b) Mao, X.; You, X.; Dai, A. *Magn. Reson. Chem.* **1989**, *27*, 836. (c) Crans, D. C.; Rithner, C. D.; Theisen, L. A. *J. Am. Chem. Soc.* **1990**, *112*, 2901. (d) Brière, K. M.; Dettman, H. D.; Detellier, C. J. *J. Magn. Reson.* **1991**, *94*, 600.

(8) (a) van Eldik, R. *Inorganic High Pressure Chemistry Kinetics and Mechanisms*; Elsevier: Amsterdam, 1986. (b) Ducommun, Y.; Merbach, A. *Inorganic High Pressure Chemistry Kinetics and Mechanisms*; van Eldik, R., Ed.; Elsevier: Amsterdam, 1986; p 69. (c) Mizuno, M.; Funahashi, S.; Nakasuka, N.; Tanaka, M. *Inorg. Chem.* **1991**, *30*, 1550 and references therein.

(9) (a) Bányai, I.; Glaser, J. *J. Am. Chem. Soc.* **1989**, *111*, 3186. (b) Bányai, I.; Glaser, J. *J. Am. Chem. Soc.* **1990**, *112*, 4703.

(10) Blixt, J.; Györi, B.; Glaser, J. *J. Am. Chem. Soc.* **1989**, *111*, 7784.

(11) Blixt, J.; Dubey, R. K.; Glaser, J. *Inorg. Chem.* **1991**, *30*, 2824.

(12) (a) Huang, Y.; Bodenhausen, G.; Ernst, R. R. *J. Am. Chem. Soc.* **1981**, *103*, 6988. (b) Ball, G. E.; Mann, B. E. *J. Chem. Soc., Chem. Commun.* **1992**, 561.

(13) (a) Biedermann, G. *Ark. Kemi* **1953**, *5*, 441. (b) Glaser, J. Ph. D. Thesis, KTH (The Royal Institute of Technology), Stockholm, 1981; p 15.

(14) Dechter, J. J.; Zink, J. I. *J. Am. Chem. Soc.* **1975**, *97*, 2937.

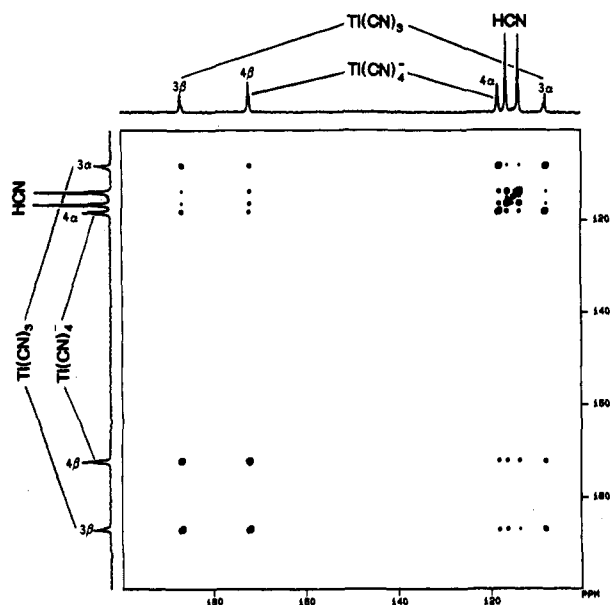


**Figure 1.**  $^{13}\text{C}$  NMR 2D EXSY spectrum (100 MHz) of an aqueous solution containing  $\text{Tl}(\text{CN})_3$ ,  $\text{Tl}(\text{CN})_4^-$ , and  $\text{HCN}$ . The thallium spin labels the energy levels of the  $^{13}\text{C}$  nuclei with  $\alpha$  (abbreviated as  $3\alpha$  for  $\text{Tl}(\text{CN})_3$  and  $4\alpha$  for  $\text{Tl}(\text{CN})_4^-$ ) and  $\beta$ . Also, the  $^{13}\text{C}$  -  $^1\text{H}$  spin-spin coupling in  $\text{HCN}$  is observed because of the very slow proton exchange with the bulk water.<sup>21</sup>  $T = 25^\circ\text{C}$ ;  $\tau_m = 35$  ms; 256 incremented experiments, each consisting of 128 scans and collected in 2K data points; relaxation delay time = 7.5 s. Fourier transformation was performed in 2K $\times$ 2K points. Weighting function in  $f_2$  is Gaussian and in  $f_1$  is a cosine function. The chemical shifts are given toward higher frequency from TMS. This spectrum, in connection with the zero mixing time experiment, was used for the calculation of the rate matrix (*cf.* text). The data were smoothed and base line corrected.

flip angle  $\sim 90^\circ$  (25  $\mu\text{s}$ ), relaxation delay time = 7.5 s, DR = 16 Hz/point, NS = 80. The chemical shifts are reported in ppm toward higher frequency with respect to an external water-soluble sodium derivative of TMS.

Some additional experimental details are given in the figure captions for Figures 1 and 3. Quantitative evaluation of the 2D EXSY peaks was performed using standard Bruker software. Horizontal and vertical slices were found to give similar results and were used instead of peak integrals.

## Results

Generally, no exchange broadening has been observed in one-dimensional  $^{13}\text{C}$  or  $^{205}\text{Tl}$  NMR spectra at room temperature. A typical  $^{13}\text{C}$  NMR 2D EXSY spectrum is shown in Figure 1. Mixing time of  $\tau_m = 35$  ms allowed the development of all relevant cross and auto peaks. (Auto peaks are generated between the lines of the same doublet.) Buildup curves for the different  $^{13}\text{C}$  NMR signals are presented in Figure 2, and a  $^{205}\text{Tl}$  EXSY spectrum is shown in Figure 3.

## Discussion

**$^{13}\text{C}$  NMR.** An inherent feature of the  $^{13}\text{C}$  NMR spectrum is that the cyanides coordinated to thallium (spin =  $1/2$ ) appear as doublets with unusually large (several kilohertz) splitting.<sup>10</sup> This large separation of  $^{13}\text{C}$  NMR lines expands the limits of the slow exchange regime. The most striking feature of this spectrum is the large intensity difference within some cross peak doublets, e.g., the  $3\alpha$ - $4\alpha$  peak is more enhanced than  $3\alpha$ - $4\beta$ .

By systematic incrementation of the mixing time, we obtained the buildup curves for the different peaks in the EXSY spectra (Figure 2).<sup>15</sup> From these curves, the dominant transfer of

(15) For sensitivity reasons, the  $\text{HCN}$  signal was  $^1\text{H}$  decoupled at all times during these experiments. From a separate 1D experiment it was found that under broad-band  $^1\text{H}$ -decoupling the steady-state  $^{13}\text{C}$ - $^1\text{H}$  NOE is uniformly transferred<sup>16</sup> to all the  $^{13}\text{C}$ -sites.

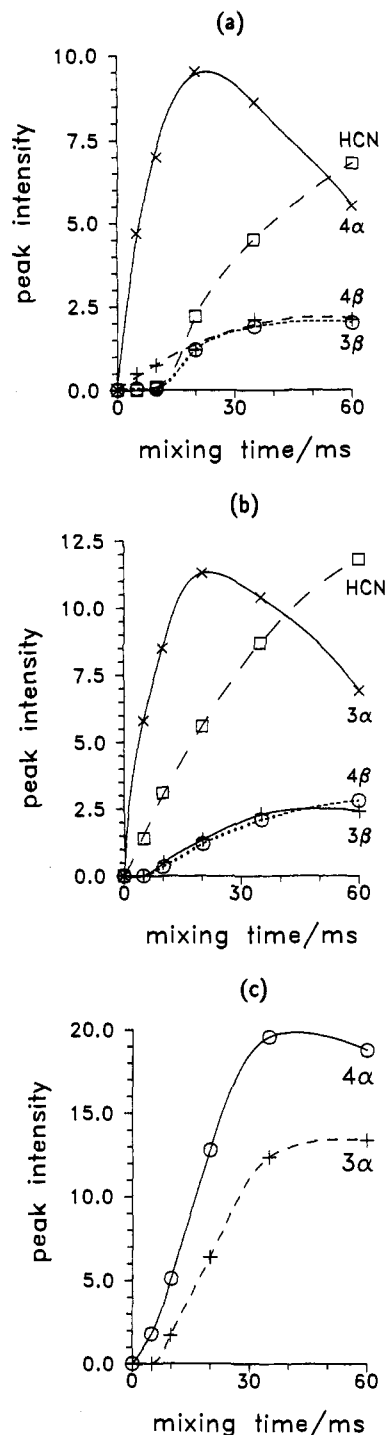
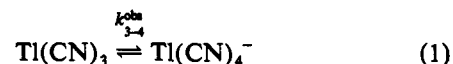


**Figure 2.**  $^{13}\text{C}$  NMR 2D EXSY buildup curves for the different exchange sites: (a)  $3\alpha$ , (b)  $4\alpha$ , and (c)  $\text{HCN}$ . The experimental points were obtained by recording spectra at varying mixing times,  $\tau_m$ .

magnetization by chemical exchange is between the following two sites:



The  $4\alpha$ - $4\beta$  auto peak and the  $4\alpha$ - $3\beta$  cross peak follow each other: both appear after a short induction period and become constant after 35 ms. The  $4\alpha$ - $\text{HCN}$  peak increases until it reaches its maximum at about 120 ms.<sup>17</sup>

For the quantitative exchange matrix analysis we performed a reference experiment with  $\tau_m = 0$  and evaluated the normalized

(16) Batta, Gy.; Kóvér, K. E.; Székely, Z.; Sztaricskai, F. *J. Am. Chem. Soc.* 1992, 114, 2757.

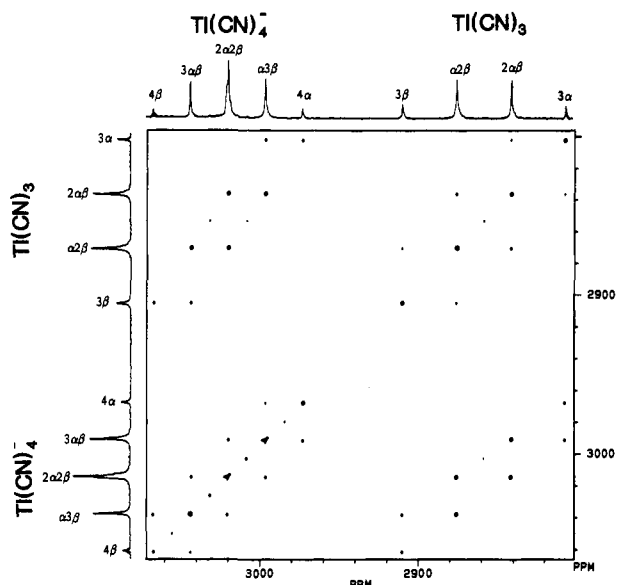


**Figure 3.**  $^{205}\text{Tl}$  NMR 2D EXSY spectrum (231 MHz) of an aqueous solution containing  $\text{Tl}(\text{CN})_3$ ,  $\text{Tl}(\text{CN})_4^-$ , and  $\text{HCN}$ . On the 1D spectra, the distribution of the  $^{13}\text{C}$  spins among the  $\alpha$  and  $\beta$  spin states at each magnetic site of the  $\text{Tl}(\text{CN})_3$  and  $\text{Tl}(\text{CN})_4^-$  complex is shown. (Also  $^{12}\text{C}$  satellites due to  $\sim 5\%$   $^{12}\text{CN}^-$  are visible and give rise to diagonal peaks).  $T = 25^\circ\text{C}$ ;  $\tau_m = 20$  ms; 512 incremented experiments, each consisting of 512 scans and collected in 2K data points; relaxation delay time = 0.27 s. Fourier transformation was performed in 2K $\times$ 2K points. Weighting function in  $f_2$  is Gaussian and in  $f_1$  is a cosine function. The chemical shifts are given toward higher frequency from an infinitely dilute aqueous solution of  $\text{Tl}(\text{ClO}_4)$ . This spectrum, in connection with the zero mixing time experiment, was used for the calculation of the rate matrix (cf. text). The data were smoothed and base line corrected.

35-ms experiment (Figure 1) using the eigenvalue matrix procedure.<sup>5</sup> Each signal in the  $^{13}\text{C}$  spectrum was treated as an independent exchanging site.<sup>18</sup> The cyanide exchange rates for the magnetization-transfer reactions 1–3 were found to be  $k_{3-4}^{\text{obs}} \approx 35$  s $^{-1}$  for reaction 1,  $k_{4-\text{HCN}}^{\text{obs}} = 3$  s $^{-1}$  for reaction 2,



and  $k_{3-\text{HCN}}^{\text{obs}} = 1$  s $^{-1}$  for reaction 3:



Now, we can turn back to the explanation of the low intensity of the cross peaks of the type  $3\alpha-4\beta$  as compared to  $3\alpha-4\alpha$ . A cyanide group which is bonded in a complex is labeled by the pertinent Tl spin state  $\alpha$  or  $\beta$ . If we consider a  $^{\beta}\text{Tl}(\text{CN})_4^-$  complex, then a dissociation of one  $\text{CN}^-$  group leads to  $^{\beta}\text{Tl}(\text{CN})_3$  and thus gives rise to a  $4\beta-3\beta$  cross peak. If the leaving  $\text{CN}^-$  group (which has now lost its Tl spin label) binds to a  $^{\alpha}\text{Tl}(\text{CN})_3$  complex and forms  $^{\alpha}\text{Tl}(\text{CN})_4^-$ , then it immediately becomes  $\alpha$ -labeled and results in a  $3\alpha-4\alpha$  cross peak. Mixed  $\alpha$ - $\beta$  type cross peaks, e.g.,  $4\alpha-3\beta$ , may arise only if within the mixing time two events occur: (1) the loss of a  $\text{CN}^-$  group from  $\text{Tl}(\text{CN})_4^-$  and (2) Tl spin flip via Tl spin-lattice relaxation. This explanation is supported by the buildup curves, where, after a 5-ms induction period, evolution of a  $4\alpha-3\beta$  cross peak can be observed (Figure 2b). The corresponding buildup curves measured at lower magnetic field (5.87 T; 62.4 MHz for  $^{13}\text{C}$ )<sup>17</sup> show significantly longer induction

(17) The values for  $\tau_m > 60$  ms at 9.4 T and all values at 5.87 T were obtained from 1D-EXSY experiments using the DANTE-Z technique: (a) Boudot, D.; Canet, D.; Broudeau, J.; Boubel, J. C. *J. Magn. Reson.* 1989, 83, 423. (b) Batta, Gy.; Kövér, K. E. *Tetrahedron* 1991, 3535.

(18) An internal consistency of the data was proved by the fact that the population ratios could be calculated from the forward and backward exchange rates and agreed within 5% with the known composition of the solution.

period, 80 ms. This striking difference can be explained by the larger contribution of the chemical shift anisotropy (CSA) mechanism to the thallium-205  $\tau_1$  relaxation at the higher field (other relaxation mechanisms and chemical exchange rates are field-independent). It is known from separate  $^{205}\text{Tl}$  NMR measurements<sup>19a</sup> that the  $\text{Tl}(\text{CN})_3$  complex is relaxed much more efficiently by the CSA mechanism than  $\text{Tl}(\text{CN})_4^-$ . Also, we have found that the relaxation time of thallium in  $\text{Tl}(\text{CN})_4^-$  (*vide infra*) is several times longer than the time range of the studied chemical exchange processes. Therefore, the dissociation of  $\text{CN}^-$  from  $\text{Tl}(\text{CN})_4^-$  must precede the relaxation of the thallium nucleus, which occurs predominantly at the  $\text{Tl}(\text{CN})_3$  complex. The apparent rate constant obtained by the matrix analysis is  $k_{3\alpha-4\beta} < 1$  s $^{-1}$ . This low apparent rate is due to the fact that this is a multiple-step (indirect) process: the Tl relaxation within the  $\text{Tl}(\text{CN})_3$  complex is contiguously interrupted by the formation, via reaction 1, of  $\text{Tl}(\text{CN})_4^-$ , for which the Tl relaxation is less efficient.

Also, the auto peaks of the  $^{13}\text{C}$ -EXSY spectrum can be evaluated and lead to an indirect estimation of the pertinent  $^{205}\text{Tl}$  spin-lattice relaxation times: 50 ms for  $\text{Tl}(\text{CN})_3$  and 210 ms for  $\text{Tl}(\text{CN})_4^-$ .<sup>20</sup> This method of calculation of relaxation times has been suggested by Ernst et al.<sup>12a</sup> and can be useful for nuclei which are difficult to detect in a direct way.

For  $\text{HCN}$ , reaction 2 can be considered. It represents a *nonmutual exchange* and gives four cross peaks within the  $4\alpha$ ,  $4\beta$  and  $^{\alpha}\text{HCN}$ ,  $^{\beta}\text{HCN}$  cross peak cluster. All of these have equal intensities due to equal chemical reactivity of the participating sites, which is independent of the nuclear spin state.

Reaction 3 gives rise to a similar cross peak pattern. However, this reaction is probably indirect and proceeds mainly through reactions 1 and 2, as can be inferred from the induction period in buildup curves for the  $\text{Tl}(\text{CN})_3$  -  $\text{HCN}$  cross peaks.

The auto peaks of the  $\text{HCN}$  sites seem to be connected with the proton exchange (and perhaps also proton relaxation) of the  $\text{HCN}$  molecule. The former was recently studied,<sup>21</sup> and the proton exchange rate constant between  $\text{HCN}$  and bulk  $\text{H}_2\text{O}$  was determined,  $k_0 \approx 30$  s $^{-1}$ .

**$^{205}\text{Tl}$  NMR.** In order to obtain complementary information on the dynamics of the system, we also recorded  $^{205}\text{Tl}$  NMR EXSY spectra of the same solution (Figure 3). In these spectra,  $\text{Tl}(\text{CN})_4^-$  appears as a pentet and  $\text{Tl}(\text{CN})_3$  as a quartet. It can be concluded by inspection of the tilted appearance of the cross peak region that the latter originate from reactions which include migration of only a single cyanide ion. Certainly, this result could be expected since a simultaneous transfer of more than one cyanide ion is improbable. Still, the fact that such information can be obtained from a single NMR experiment shows the predictive potential of the method. Quantitative evaluation led to the rate constant  $k_{3-4}^{\text{obs}} \approx 50$  s $^{-1}$ ,<sup>22</sup> in acceptable agreement with the  $^{13}\text{C}$  EXSY data ( $\approx 35$  s $^{-1}$ ).

The auto peak region around the diagonal is an interesting part of the  $^{205}\text{Tl}$  NMR 2D EXSY spectrum. These peaks cannot originate from the  $^{13}\text{C}$   $T_1$  relaxation since the apparent  $^{13}\text{C}$  relaxation time in this solution is  $\sim 4.5$  s (from  $^{13}\text{C}$  NMR inversion-recovery experiments). This may give a contribution of only  $\sim 0.1$  Hz to the exchange rates among the sites responsible

(19) (a) Bányai, I.; Glaser, J., to be published. (b) Blixt, J.; Glaser, J.; Persson, I.; Sandström, M., to be published.

(20) These include, probably, contributions from multistep exchange processes, as can be inferred from the induction delay in the  $4\alpha-4\beta$  buildup curve (cf. the discussion of the  $4\alpha-3\beta$  cross peak). Relaxation rate of Tl in, e.g.,  $\text{Tl}(\text{CN})_3$ ,  $1/2R \sim 10$  s $^{-1}$ , gives  $\tau_1 \sim 50$  ms (for theoretical treatment, cf. ref 3b).

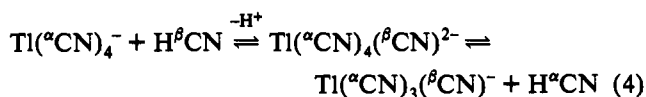
(21) Bányai, I.; Blixt, J.; Glaser, J.; Toth, I. *Acta Chem. Scand.* 1992, 46, 142. The present study was performed at  $[\text{ClO}_4^-]_{\text{tot}} = 4$  M, i.e., slightly higher than that in the cited reference. The relaxation time,  $\tau_1$ , of  $^1\text{H}$  in  $\text{HCN}$  in the present ionic medium (or close to) is not known.

(22) The rate constants from  $^{205}\text{Tl}$  NMR EXSY were obtained from the elements of the rate matrix, considering the probabilities of the different exchange reactions.

Table I. Possible Cyanide Exchange Pathways and the Resulting Cross and Auto Peaks

	chemical reaction		causes peaks in		
			<sup>13</sup> C 2D EXSY	<sup>205</sup> Tl 2D EXSY	
a	Tl(CN) <sub>3</sub> + Tl(CN) <sub>4</sub> <sup>-</sup>	⇌	Tl(CN) <sub>4</sub> <sup>-</sup> + Tl(CN) <sub>3</sub>	3α-4α, 3β-4β	cross peaks
b	Tl(CN) <sub>3</sub> + HCN	⇌	Tl(CN) <sub>3</sub> + HCN	3α-HCN, 3β-HCN	Tl(CN) <sub>3</sub> auto peaks
c	Tl(CN) <sub>3</sub> + HCN	⇌	Tl(CN) <sub>4</sub> <sup>-</sup> + H <sup>+</sup>	3α-4α, 3β-4β	cross peaks
d	Tl(CN) <sub>4</sub> <sup>-</sup> + HCN	⇌	Tl(CN) <sub>4</sub> <sup>-</sup> + HCN	4α-HCN, 4β-HCN	Tl(CN) <sub>4</sub> <sup>-</sup> auto peaks
e	Tl(CN) <sub>3</sub> + Tl(CN) <sub>3</sub>	⇌	Tl(CN) <sub>2</sub> <sup>+</sup> + Tl(CN) <sub>4</sub> <sup>-</sup>	3α-4α, 3β-4β	cross peaks
f	Tl(CN) <sub>4</sub> <sup>-</sup> + Tl(CN) <sub>4</sub> <sup>-</sup>	⇌ <sup>+H<sup>+</sup></sup>	Tl(CN) <sub>3</sub> + Tl(CN) <sub>4</sub> <sup>-</sup> + HCN	3α-4α, 3β-4β 4α-HCN, 4β-HCN	cross and auto peaks

for the auto peaks. The quantitative evaluation of these peaks for the Tl(CN)<sub>4</sub><sup>-</sup> complex gave rate constant of ~2 s<sup>-1</sup>. Thus, these peaks cannot be generated by <sup>13</sup>C relaxation but rather are the result of a chemical exchange process. Moreover, since only auto peaks originating from a replacement of one <sup>α</sup>CN<sup>-</sup> by one <sup>β</sup>CN<sup>-</sup> (or vice versa) are present, they may represent reaction 2, written as:<sup>23,24</sup>



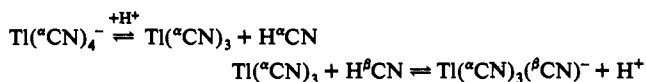
The rate constant obtained from the <sup>205</sup>Tl EXSY auto peaks (~2 s<sup>-1</sup>) is of the same order of magnitude as the rate constant  $k_{4\text{-HCN}}^{\text{obs}}$  (~3 s<sup>-1</sup>) obtained from the cross peaks of the <sup>13</sup>C EXSY spectrum. Similar ligand exchange reaction with associative mechanism was observed previously for the thallium(III) bromide system, where a small amount of TlBr<sub>3</sub><sup>2-</sup> complex was found.<sup>9b</sup>

Analogously, the auto peaks of Tl(CN)<sub>3</sub> may originate from reaction 3. Indeed, the rate constant obtained from the <sup>205</sup>Tl EXSY auto peaks (~2 s<sup>-1</sup>) is close to the rate constant  $k_{3\text{-HCN}}^{\text{obs}} \approx 1 \text{ s}^{-1}$  obtained from <sup>13</sup>C EXSY.

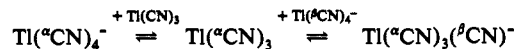
Generally, only the direct cyanide exchange reactions shown in Table I have to be considered in this case. This table has diagnostic value for determining reaction pathways. For example, if only reaction a occurs, the 3α-HCN peak should not exist. If only reaction c occurs, the peaks 3α-4α and 4α-HCN should have equal intensity. Since  $k_{3\text{-4}}^{\text{obs}}$  (from <sup>13</sup>C EXSY) ≈  $k_{3\text{-4}}^{\text{obs}}$  (from <sup>205</sup>Tl EXSY) (*vide supra*), reaction a (or possibly e) dominates the cyanide exchange between the two thallium complexes. This is a rare *intermolecular mutual exchange* process, where the two complex species approach each other and exchange a ligand (*cf.* ref 9).

(23) Note, that the labeling of <sup>α</sup>CN and <sup>β</sup>CN in the <sup>205</sup>Tl NMR spectroscopic part should not be confused with <sup>α</sup>Tl and <sup>β</sup>Tl discussed previously for <sup>13</sup>C NMR spectroscopy.

(24) The alternative, dissociative reaction,



could also be possible. However, we known from <sup>13</sup>C EXSY experiments that reaction 3 is very slow. Therefore, the path 4 is probably correct. Also, two consecutive reactions 1, *e.g.*,



can generate the 4α-3αβ auto peak. Other multistep paths cannot be excluded but would be significantly slower.

The auto peaks of the Tl(CN)<sub>3</sub> complex in the <sup>205</sup>Tl EXSY spectra can be caused only by reaction b. This reaction is indirect (*vide supra*).

A more detailed discussion of the chemical exchange pathways and reaction mechanisms demands a variation of the solution composition and the temperature,<sup>19a</sup> as well as structural information on the studied species,<sup>19b</sup> and is outside the scope of the present paper.

### Conclusions

In this paper we present some peculiar aspects of the 2D EXSY technique using the combined power of two NMR active, spin = 1/2 nuclei for a three-component chemical system, Tl(III)-CN<sup>-</sup>-H<sup>+</sup>, in aqueous solution. The well-resolved heteronuclear spin-spin couplings result in six exchanging sites for <sup>13</sup>C NMR (Figure 1) and nine for <sup>205</sup>Tl NMR (Figure 3). 2D exchange spectroscopy provides an overview of the exchange reactions and gives their rates. Interesting and in some cases otherwise not accessible information on the equilibrium dynamics can be obtained by quantitative interpretation of cross and auto peaks. The presence of the "spy nuclei", <sup>205</sup>Tl and <sup>1</sup>H for <sup>13</sup>C NMR and <sup>13</sup>C for <sup>205</sup>Tl NMR, serves as an additional information source. In a particular case, we found that the field dependence of CSA relaxation may give insight into the microscopic order of consecutive migration processes.

We found that <sup>205</sup>Tl EXSY results suffer from larger errors compared to its <sup>13</sup>C counterpart because of the inherent difficulties of <sup>205</sup>Tl NMR spectroscopy. For example, the large spectral window (70 kHz) causes unavoidable phase errors and poor digital resolution (~60 Hz/point). We have compared some of the rate constants presented above with the corresponding constants obtained from selective <sup>205</sup>Tl NMR 1D magnetization-transfer experiments.<sup>19a</sup> The two methods gave similar results, but it could be shown that the accuracy of the obtained rate constants is better for the 1D method. Nevertheless, the strength of the 2D EXSY lies in its ability to provide an overview of the different kinetic pathways from a single solution and to selectively excite even closely spaced signals (here 4α and HCN, *cf.* Figure 1).

**Acknowledgment.** The continuous financial support from the Swedish Natural Science Research Council (NFR) and the grant from the Hungarian National Scientific Research Foundation (OTKA 1144, 1724) are gratefully acknowledged. We are grateful to the Swedish Institute and to the Wenner-Gren Center Foundation for the fellowships covering the stay of I.B. in Stockholm.